Journal of Applied Mechanical Engineering
ISSN: 2168-9873

Badreddine et al., J Appl Mech Eng 2016, 5:5
DOI: 10.4172/2168-9873.1000225

Research Article | Open Access

New Approach of Metals Ductility in Tensile Test

Badreddine R*[1], Abderrazak D[1] and Kheireddine S[2]

[1]*Departement de metallurgie et génie des materiaux, laboratoire de metallurgie et genie des materiaux, universite badjimokhtar 23000 Annaba*
[2]*Research Center in Industrial Technologies, CRTI P. O. Box 64, Cheraga 16014 Algiers, Algeria*

Abstract

Ductility is the ability of a material to deform plastically before rupture. This is an important feature in shaping because it helps to define the behavior of materials. Ductility is therefore essential to know and thus determine to anticipate the behavior of materials in various situations of stress. Ductility is commonly defined by the two parameters A elongation (in percent) or necking Z (in percent) with:

A(%) = ΔL/L_0(%) = (L_1-L_0)/L_0(%) and Z(%) = ΔS/S_0(%) = (S_0-S_1)/S_0(%)

These two parameters are determined from tensile tests on standard specimens.

We will focus on the study and analysis of ductility using the tensile test.

However these two indicators (A) and (Z) of the ductility may present deficiencies (contradictions) in the interpretation of the ductility in case where for two samples (1) and (2) with same original dimensions (Lo) and (So) and different composition we could have : A1>A2 and Z1<Z2 or A1<A2 and Z1>Z2.

These two cases show the anomaly between A and Z in the assessment of the ductility, in fact in the first case the sample (1) is more ductile than the sample (2) in terms of elongation (A) is less ductile necking in terms of (Z) against the 2nd case we find the opposite behavior; it is this inconsistency that we will approach the ductility by introducing a parameter which will be called ductility (D) which takes into account the elongation and necking in a single formulation. In fact, (D) could remedy this deficiency involving computational approaches by activating the settings of the length (L) and Section (S) across the diameter (d) together in a first approach and to other computational approaches that take into account the elongation A and the neck.

Keywords: Ductility; Elongation; Necking; Tensile; Approach

Introduction

Ductility is the ability of a material to deform plastically before rupture. This is an important feature in shaping because it helps to define the behavior of materials. Ductility is therefore essential to know and thus determine to anticipate the behavior of materials in various situations of stress. Ductility is commonly defined by the two parameters A elongation (in percent) or necking Z (in percent) with:

$$A(\%) = \frac{\Delta L}{L_0}(\%) = \frac{L_1 - L_0}{L_0}(\%) \quad and$$

$$Z(\%) = \frac{\Delta S}{S_0}(\%) = \frac{S_0 - S_1}{S_0}(\%)$$

These two parameters are determined from tensile tests on standard specimens.

We will focus on the study and analysis of ductility using the tensile test.

However these two indicators (A) and (Z) of the ductility may present deficiencies (contradictions) in the interpretation of the ductility in case where for two samples (1) and (2) with same original dimensions (Lo) and (So) and different composition we could have:

$A_1>A_2$ and $Z_1<Z_2$

Or $A_1<A_2$ and $Z_1>Z_2$

These two cases show the anomaly between A and Z in the assessment of the ductility, in fact in the first case the sample (1) is more ductile than the sample (2) in terms of elongation (A) and less ductile in terms of necking (Z); in the 2nd case we find the opposite behavior; it is this inconsistency that we will approach the ductility by introducing a parameter which will be called ductility (D_1) which takes into account the elongation and necking in a single formulation. In fact, (D_1) could remedy this deficiency involving computational approaches by activating the settings of the length (L) and Section (S) across the diameter (d) together [1-20].

Materials and Methods

Ductility modeling and approaches of metals

Highlighting the contradiction of the ductility value between the parameters A(%) and Z(%): The anomaly of appreciation of ductility that we expose, concerned the contradiction between the percent elongation parameter A(%), and the percent necking Z parameter (%). This anomaly is confirmed by numerous examples; among metals and alloys defined according to the American standard AISI and ASTM Table 1, some of them confirmed the contradiction between A(%) and Z(%) (Table 1) [21-40].

So this contradiction leads us to propose modeling approaches of ductility to remedy this inconsistency and thus give a more meaningful assessment of the ductility by inter reactive factors such as the length, section and through which the diameter during deformation (Table 2).

***Corresponding author:** Badreddine R, Department de métallurgie et genie des materiaux, laboratoire de métallurgie et genie des matériaux, université badjimokhtar 23000 Annaba, Tel: +213 661 04 08 93; E-mail: bregaiguia@yahoo.fr

Received June 14, 2016; **Accepted** June 30, 2016; **Published** July 03, 2016

Citation: Badreddine R, Abderrazak D, Kheireddine S (2016) New Approach of Metals Ductility in Tensile Test. J Appl Mech Eng 5: 225. doi: 10.4172/2168-9873.1000225

Citation: Badreddine R, Abderrazak D, Kheireddine S (2016) New Approach of Metals Ductility in Tensile Test. J Appl Mech Eng 5: 225. doi: 10.4172/2168-9873.1000225

	E (Gpa)	Rp (Mpa)	Rm (Mpa)	A%	Z%
Ductile Iron A536 (6545-12)	159	334	448	15	19.8
Rolled AISI 1020	203	260	441	36	61
ASTM A514, T1	208	724	807	20	66
Ni Maraging Steel (250)	186	1791	1860	8	56
Aluminium 2024 –T4	3.1	303	476	20	35

Table 1: Mechanical properties of some metals [57].

Metals	A	Z
Ductile Iron A536 (65-45-12) Ni Maraging Steel (250)	15 8	19.8 56
Rolled AISI 1020 ASTM A514 , T1	36 20	61 66
Ni Maraging Steel (250) Aluminium 2024-T4	8 20	56 35

Table 2: Examples of metals with a contradiction between the ductility parameters A (%) and Z (%).

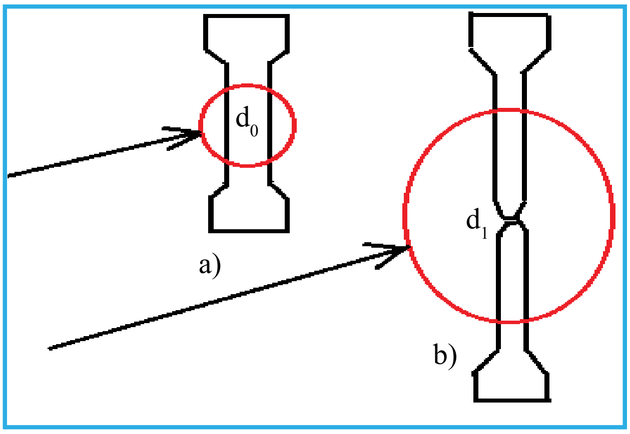

Figure 1: a) Specimen before tensile test; b) Specimen after tensile test.

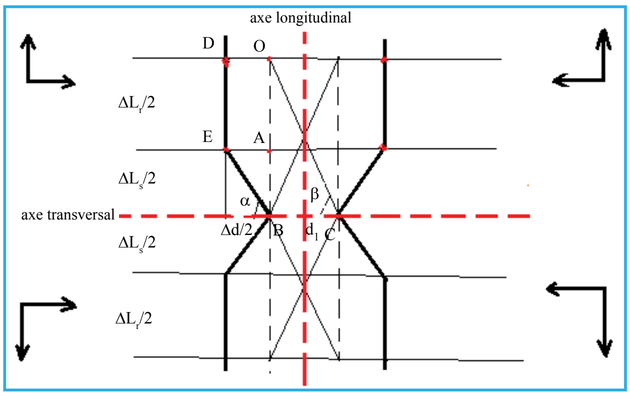

Figure 2: Geometric representation of the D_1 approach on a specimen after breaking.

Approach 1: Geometric modeling approach ductility according to the elongation and diameter necking

This is a standardized tensile specimen with respectively Lo, So length and initial section L_1 and S_1 length and section after tensile test. It is known that the elongation consists of two separate elongations including one distributed almost uniformly over the entire length of the test piece, while the other is located at the point of necking [41,42]. Uniform elongation is calculated by expressing the volume of the specimen between the landmarks of the test piece is not changed by this elongation, then:

$$\left[\left(\frac{d_0}{d_1}\right)^2 1\right]x100\% \qquad (1)$$

Or: d_0 is the diameter of the specimen before the tensile test and d_1 after breaking.

b(%): lengthening of necking, established by the difference:

$$b(\%) = A(\%) - a(\%) \qquad (2)$$

A(%): Total elongation measured on standard test specimen.

Assuming that $A = A_R + A_S$.

We focus on the study of uniform elongation and elongation of necking during the tensile deformation.

It discusses this approach by a geometric representation formulation of these parameters enabled.

We consider a standard tensile bar with respectively:

L_o and S_o: the length and the section before tensile test.

L_1 and S_1: the length and the section after tensile test.

By analyzing necking area, it is noted that:

Longer necking which is ΔL_S is a line that develops in the direction of the loading axis.

Necking which is the ratio of ΔS and initial section S_0 is represented in our approach by the difference of initial diameter d_0 and diameter after breaking d_1.

In the work that follows, we will focus our approach on the specimen deformation area (Figure 1).

According to Figure 2, it is assumed that:

- The test piece is perfectly symmetrical on both sides of the longitudinal and transverse axes.

- After the tensile test piece halves of both sides with respect to the break line (necking) are symmetrical.

- The breaking line (necking) is mingled with the transverse axis.

- The variation of the section profile in the necked area is made along a straight right from the beginning of the necking to failure.

- We introduced the concept of necking bearing represented by the oblique line EB represents the profile of the evolution of reduced diameter.

- We introduce the notion of necking angle (tgα) which is the angle resulting from the intersection of the transverse confused with BC and EB bearing.

- We introduced the concept of 1/2 ductility triangle whose base is necking diameter and height is total elongation.

- We introduced the concept of 1/2 ductility angle β formed by the intersection of the base of the triangle (diameter necking) and the hypotenuse OC.

Citation: Badreddine R, Abderrazak D, Kheireddine S (2016) New Approach of Metals Ductility in Tensile Test. J Appl Mech Eng 5: 225. doi: 10.4172/2168-9873.1000225

We note in Figure 2 that we have:

04 geometric representations highlighting $\frac{\Delta L_r}{2}$ $\frac{\Delta L_S}{2}$ et $\frac{\Delta d}{2}$.

Symmetrically, 02-02 relative to longitudinal and transverse axes.

However, we will focus our approach of calculating the approach D_1 on geometric representation of the left upper half specimen. In the Figure 2 we see the necking profile across the necking bearing EB that means we see the profile of the evolution of strain in term of elongation and diameter reduction necking d_1 until the breaking [43-47].

Calculation Method of D_1 Ductility Approach

Either the diagram of portion 1(3);

Note from the geometry:

$\frac{\Delta L_r}{2}$ is the uniform elongation of the portion 1.

$\frac{\Delta L_s}{2}$ is the extension of the constriction portion 1.

With: ΔL_S total elongation at necking.

$\frac{\Delta d}{2}$: is the difference between initial and final diameter of the portion 1.

According to Figure 3 we have,

The point O:

$$\frac{\Delta L}{2} = 0 \text{ et } \frac{\Delta d}{2} = 0$$

With $\frac{\Delta L}{2}$: the total elongation of the portion 1 of the specimen and Δd: Δd the variation of the diameter.

This is the initial state at time t = 0 before tensile test.

At point A: There, there's uniform elongation but there is no necking as $\Delta d = 0$.

Consequently the total elongation of the portion 1 is: $\frac{\Delta L}{2} = \frac{\Delta L_r}{2}$

At point B:

We have uniform elongation and necking because there's $\Delta d \neq 0$

Consequently the total elongation of the portion 1 is:

$$\frac{\Delta L}{2} = \frac{\Delta L_r}{2} + \frac{\Delta L_S}{2}$$

With: $\frac{\Delta L_r}{2}$ et $\frac{\Delta L_S}{2}$ respectively: uniform elongation and necking elongation.

We note already in Figure 2 that: the necking elongation ΔL_S can be calculated as follows:

$$tg\alpha = \frac{\frac{\Delta L_S}{2}}{\frac{\Delta d}{2}} = \frac{\Delta L_S}{\Delta d} \tag{3}$$

The angle β is introduced between the transverse which coincides with the necking diameter and the slant segment passing through the point O and the end of the necking diameter in point C introducing the tangent of the angle β:

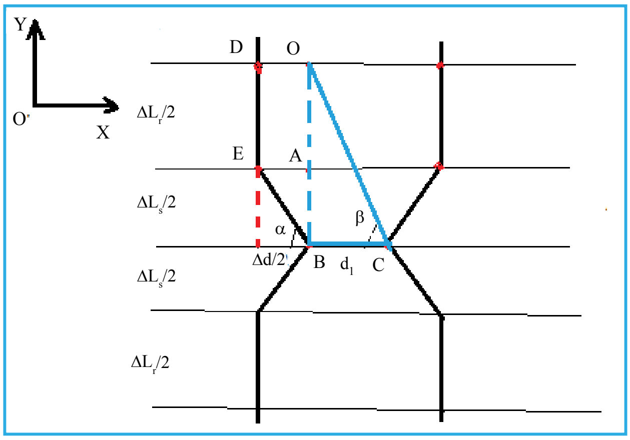

Figure 3: Representation of the D_1 approach of the upper left half specimen (portion 1).

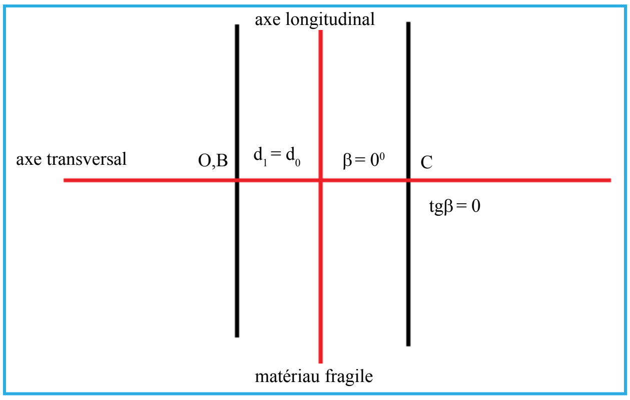

Figure 4: Geometric representation of the D_1 approach on a test specimen of brittle material.

$$tg\beta = \frac{OB}{BC} = \frac{OB}{d_1} = \frac{OA + AB}{d_1} = \frac{\frac{\Delta L_r}{2} + \frac{\Delta L_S}{2}}{d_1} = \frac{\Delta L}{2d_1}$$

$$\text{So } tg\beta = \frac{\Delta L}{2d_1} \tag{4}$$

Note that the β angle is between 0° and 90°: $0^0 \leq \widehat{OCB} \leq 90^0$

$$tg0^o = \frac{0}{1} = 0 \text{ et } tg90^o = \frac{1}{0} = \infty$$

Indeed 0° corresponds to the initial state before tensile test or the ductility of the material is zero.

At 90° is the condition for which the ductility of the material is infinite.

Interpretation

We note from Figure 4 that:

When β = 0° this means that the material is brittle because its ductility expressed $tg\beta$ is zero.

When β = 90° (Figure 5), it means that the material is ideally plastic that is to say the material is infinitely superplastic because its ductility expressed by $tg\beta$ approaches infinity.

We see that $tg\beta$ is a credible indicator of ductility because it activates simultaneously the elongation ΔL and the final necking diameter d_1 (Figure 6).

This formulation is interesting because it is based on the values of the elongation ΔL and the final necking diameter d_1 which are essential variables in the determination of the ductility of a material.

Among others we note that conventional formulas of ductility represented by the percent elongation A and the necking percent Z are dependent on these 02 values, in fact elongation percent A is a function of only ΔL and necking Z is a function of the necking section S_1 it means that Z is a function of necking diameter d_1 [48-57].

We shall agree to say, therefore, that our approach of ductility through the tangent of the angle β gives a better description of the state of ductility of material than conventional parameters A and Z.

Checking the formula of ductility approach $tg\beta = \frac{\Delta L}{2d_1}$ of portion

When, $tg\beta = 0$ this corresponds to $\beta = 0° \Rightarrow \frac{\Delta L}{2d_1} = 0$

We deduce: $\Delta L=0$ et $d_1 = d_0$.

This is the case of a brittle material whose ductility is zero.

When $tg\beta = \infty$ it corresponds to $\beta = 90° \Rightarrow \frac{\Delta L}{2d_1} \to \infty$ we deduce: $\Delta L >> 0$ et $d_1 \to 0$.

This is the case of a ductile material with ideally infinite ductility it

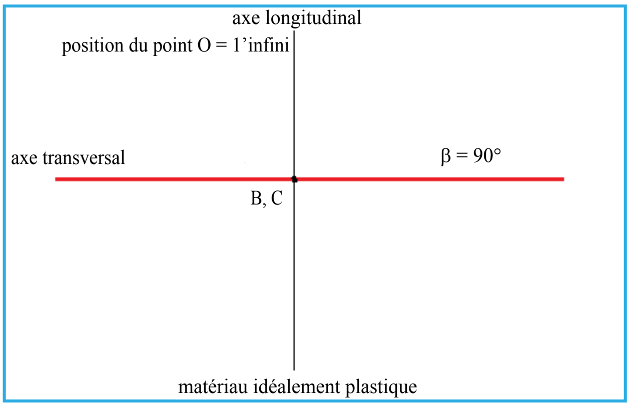

Figure 5: Geometric representation of the D_1 approach on a test specimen of an ideal plastic material.

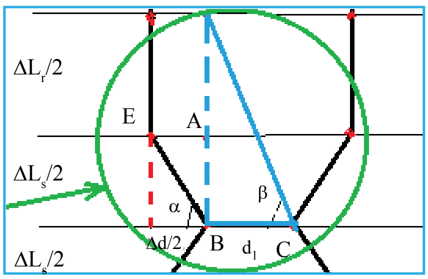

Figure 6: Angle β representation in function of the elongation and diameter necking d_1.

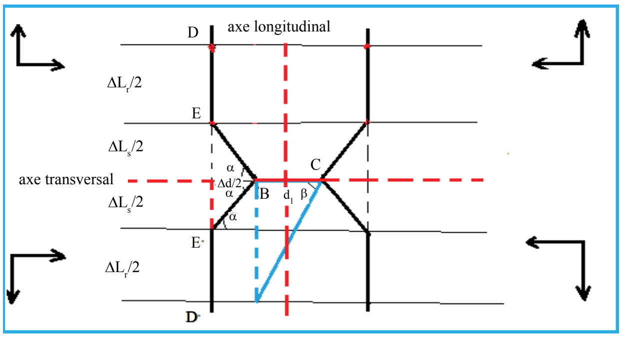

Figure 7: Representation of the D_1 approach of the lower left half specimen.

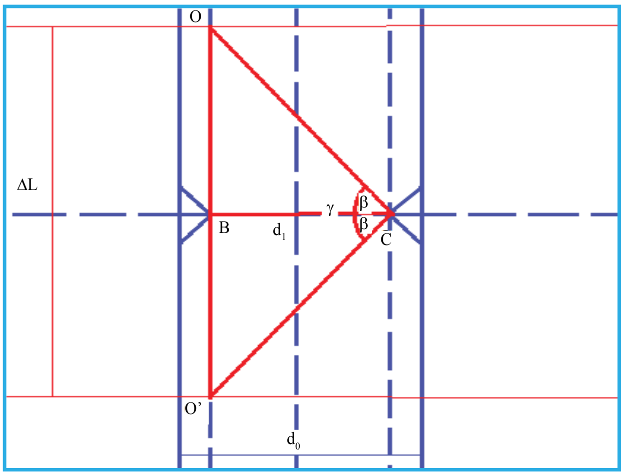

Figure 8: Representation of the D_1 approach for left side specimen.

is concluded from our approach $tg\beta = \frac{\Delta L}{2d_1}$ the ductility of superplastic metallic materials and plastic is between 0 and infinity.

We conclude $tg\beta = \frac{\Delta L}{2d_1}$ may be representative of the ductility of any material.

To finalize our approach of ductility formula, we notice that $tg\beta$ is representative of the ductility of the upper half of specimen (Figure 3).

Based on the assumptions mentioned above, the test specimen is perfectly symmetrical on both sides of the axes, thus to have the total ductility, it is appropriate to add the ductility of the lower half specimen (Figure 7) or multiply our parameter $tg\beta = \frac{\Delta L}{2d_1}$ by 2.

$$\text{So } D_1 = 2tg\beta = 2\frac{\Delta L}{2d_1} = \frac{\Delta L}{d_1} \qquad (5)$$

With ΔL: total elongation and d_1: necking diameter.

So we see that the total ductility triangle is isosceles shape, with basic ΔL and total height the extension of necking diameter d_1 (Figure 8).

We also note that the total angle of ductility is the angle $\gamma = 2\beta$.

We note that the ductility parameter approach $D_1 = \frac{\Delta L}{d_1}$ is an interesting and promising contribution in the interpretation of ductility. It has been confirmed by audits on 03 types of materials

Citation: Badreddine R, Abderrazak D, Kheireddine S (2016) New Approach of Metals Ductility in Tensile Test. J Appl Mech Eng 5: 225. doi: 10.4172/2168-9873.1000225

(brittle, plastic and superplastic); in the other hand it is easy to use and involves the elongation ΔL and the necking Z throughout the diameter d_1 under a single formulation.

The ductility approach $D_1 = \dfrac{\Delta L}{d_1}$ effectively solves the problem of the contradiction between A and Z concerning quantification of ductility and that is the problem targeted by the work (Figure 9).

Analysis of approach $D_1 = \dfrac{\Delta L}{d_1}$ for ductile metallic materials

To simplify the geometric representation of the D_1, we preferably used approach for the upper 1/2 specimen (Figure 10) or lower 1/2 specimen; while noting that the geometric shape relative to D_1 approach is an isosceles triangle that is the sum of 02 right triangles (rectangle triangles) perfectly identical and symmetrical and having a common base the diameter of the specimen.

According to Figure 10a shows the evolution of our approach ductility parameter from a simple tensile test on the 1/2 upper specimen.

In Figure 10, D_1 approach parameter before the beginning of the tensile test is shown by the initial state $\Delta L_r = \Delta L_s = 0$; Indeed, the elongation is zero and $\Delta d = 0$ which implies $d_1 = d_0$.

In this case: $D_1 = \dfrac{\Delta L}{d_1} = \dfrac{\Delta L}{d_0} = \dfrac{0}{d_0} = 0$

This is the typical case of brittle materials whose ductility is zero.

Figure 10b represents the beginning of the test; we note that there is a linear deformation along the longitudinal axis therefore representing the homogeneous deformation of the uniform elongation of the specimen.

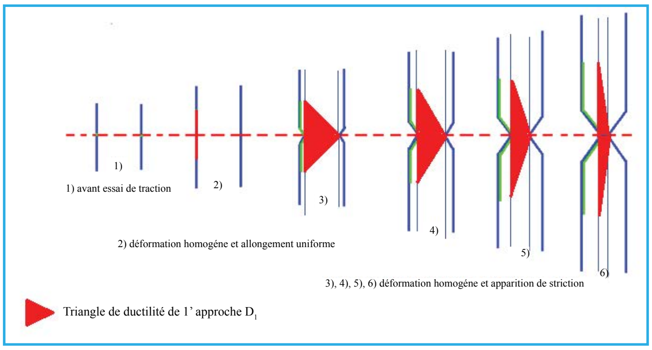

Figure 9: Geometric evolution of D_1 approach parameter on a specimen in tensile test.

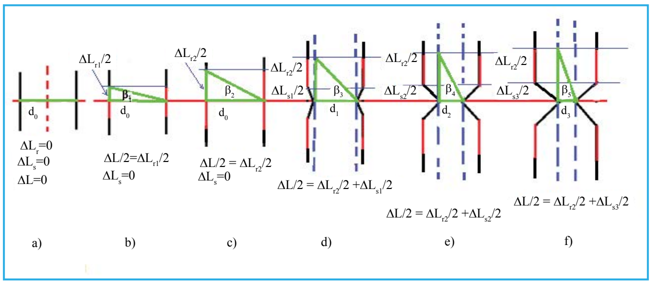

Figure 10: Different steps of evolution of the parameter D_1 on a $\frac{1}{2}$ specimen in tensile test.

The D_1 parameter in this case is based only on the uniform elongation because it is homogeneous deformation and the initial diameter d 0 because there is no necking.

$D_1 = \dfrac{\Delta L_{r1}}{d_0}$

In Figure 10c the homogeneous deformation representing uniform elongation is more pronounced than the previous but still remains in the field of homogeneous deformation, the uniform elongation ΔLr increased passing ΔL_{r2} with $\Delta L_{r2} > \Delta L_{r1}$ therefore only the uniform elongation occurs in changing the quantization ductility because necking elongation is zero and the diameter $d_1 = d_0$.

What gives us the setting $D_1 = \dfrac{\Delta L_{r2}}{d_0}$

In Figure 10d we notice the onset of necking one enters the area of the heterogeneous deformation indeed it there's diameter reduction and lengthening necking. The total elongation in this case is the sum of 02 elongations: distributed elongation and elongation necking ΔL_{s1} and the diameter d_1 which is less than d_0.

Note that the uniform elongation is constant and equals to ΔL_{r2} because it is no longer homogeneous deformation.

Where: $D_1 = \dfrac{\Delta L_{r2} + \Delta L_{s1}}{d_1}$

In Figure 10e necking is more pronounced, as necking elongation and diameter reduction are enabled, there is a slight increase in the value of the necking elongation and a decrease of the diameter from d_1 to d_2; $d_2 < d_1$.

This increase is induced by the increase in the value of the diameter reduction, that we confirm through the formula that we presented $\Delta L_s = \Delta dx\, tg\alpha$.

Indeed when Δd increases, ΔL_s also increases, which means $\Delta L_{s2} > \Delta L_{s21}$

Therefore the approach of parameter D_1 becomes equal to: $D_1 = \dfrac{\Delta L_{r2} + \Delta L_{s2}}{d_2}$

According to Figure 10f the breaking phase we are witnessing is the end of the necking so necking elongation increases $\Delta L_{s3} > \Delta L_{s2}$ and necking diameter decreases with d_3 less than d_2.

So the approach parameter will be: $D_1 = \dfrac{\Delta L_{r2} + \Delta L_{s3}}{d_3}$

We note that in general the ductility parameter $D_1 = \dfrac{\Delta L}{d_1}$ is growing throughout the tensile test and interprets perfectly plastic behavior through its 02 variables that are elongation ΔL and necking diameter d_1.

Ductility Triangle and Ductility Angle Concepts of Approach D_1

It is a specimen of a material subjected to a simple tensile test. Changes in ductility through the D_1 setting approach has been described above, however we will try to study the evolution of ductility triangle through the various phases of tensile strain. Either the 1/2 upper specimen, the mapping of the ductility is proposed to be made through the triangle by the projection on the longitudinal axis in Figure 11 which gives us the following:

Citation: Badreddine R, Abderrazak D, Kheireddine S (2016) New Approach of Metals Ductility in Tensile Test. J Appl Mech Eng 5: 225. doi: 10.4172/2168-9873.1000225

It is seen (FIG II.11) that D_1 approach parameter relating to the 1/2 specimen changes according to a right triangle whose height characterizing the elongation increases at the expense of shrinkage of diameter.

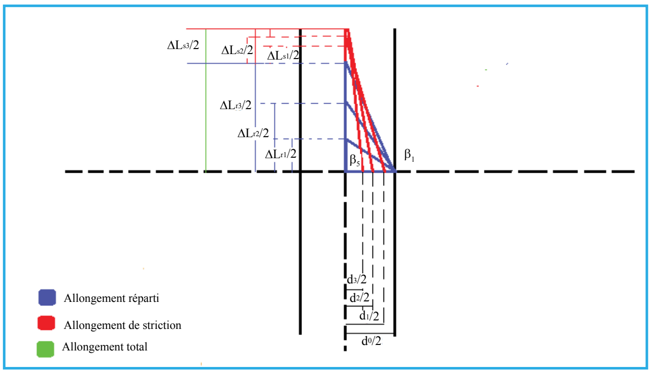

Figure 11: Evolution of shape of ductility triangle and ductility angle of the upper half specimen.

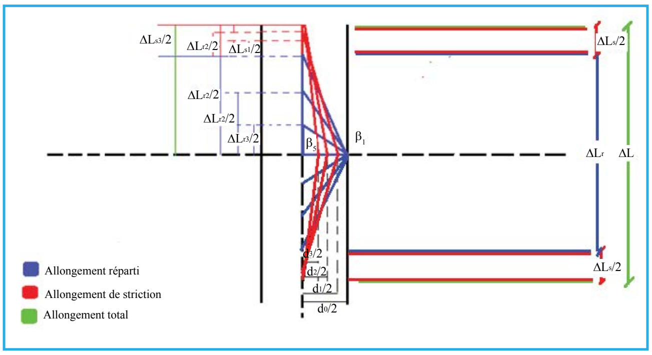

Figure 12: Evolution of shape of the ductility triangle and the ductility angle of the specimen.

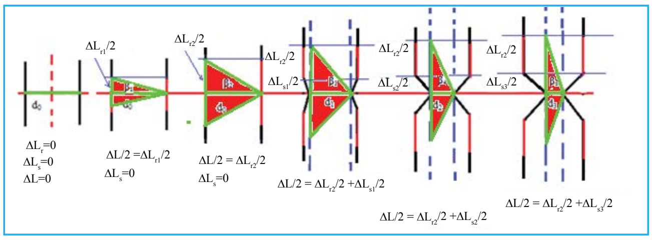

Figure 13: Geometric distribution of the D_1 approach ductility triangle.

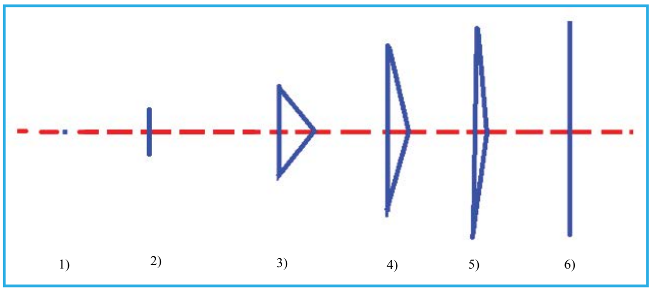

Figure 14: Different stages of evolution of ductility triangle.

This change in shape of the right triangle called ½ ductility triangle is expressed by the variation of angle of inclination β called 1/2 ductility angle.

We also note from the Figure 11, that as β increases, the ductility formulated by D_1 approach also increases and vice versa true.

Indeed it is clear that: $\beta_6 > \beta_5 > \beta_4 > \beta_3 > \beta_2 > \beta_1$.

Therefore it is concluded that the ductility of approach $D_1 = \dfrac{\Delta L}{d_1}$ on the ½ specimen is geometrically represented by a variable right triangular D_1 and this parameter is a function of the ½ β ductility angle whose value is only determining ductility relative to our approach.

Note that the parameter $D_1 = \dfrac{\Delta L}{d_1}$ is finally dimensionless.

For the entire test the geometric representation of the D_1 approach is as follows in Figure 12.

Note on Figure 13, the evolution of the isosceles triangle ductility characterizing D_1 approach; Indeed, starting from t=0 to the beginning of the homogeneous deformation ductility scales linearly along the axis of stress is the uniform elongation and to the onset of necking there is formation of a triangle isosceles which characterizes the heterogeneous deformation according to the approach D_1. This form of this triangle changes gradually as the tensile test is carried out until breaking of the specimen.

Finally we conclude that changes in the geometry of the D_1 approach operate generally as follows in the Figure 14.

Figure 14.1: No deformation, it is the initial state before tensile testing; ductility is confused to a point.

Figure 14.2: Homogeneous deformations, it is the phase of the distributed linear expansion, there is no ductility triangle.

Figures 14.3 - 14.5: Heterogeneous deformation, it is the phase of the emergence and evolution of ductility triangle according D_l approach.

Figure 14.6: The ductility triangle coincides with the vertical and corresponds to an ideal state of ductility that does not exist in reality. It operates between other than the area of the isosceles triangle is equal to $\dfrac{bh}{2}$ that is the product of base of the triangle and its 1/2 height. Therefore the area of the triangle ductility characterizing D_1 ductility approach is equal to $\dfrac{\Delta L x d_1}{2}$.

Note that the parameter $D_l = \dfrac{\Delta L}{d_1}$ is dimensionless.

Results and Discussion

To study and analyze the contradiction between the assessment parameters of ductility A(%) and Z(%) we used in our experiment iron annealed copper annealed. These (02) grades are delivered in rolled state by the precision machining company located in El-Hadjar (Annaba city).

The various test pieces in number (03) for each grade were tested in the tensile test; the different values that we identified (final length and final diameter), are used to calculate average ΔL and necking diameter for proving the contradiction.

For iron annealed, elongation is between 40 and 50, the constriction

Citation: Badreddine R, Abderrazak D, Kheireddine S (2016) New Approach of Metals Ductility in Tensile Test. J Appl Mech Eng 5: 225. doi: 10.4172/2168-9873.1000225

is 80 to 93, the hardness HRB is from 45 to 55 and its modulus of elasticity (Young) is 206000 MPa.

To develop and analyze the second step of our work, we experiment tensile test on 03 different grades of carbon steel. For each grade, we use 03 specimens. Test grades are XC18 carbon steel, XC38 and XC48. Ductility values of the above-mentioned steels is known because of the carbon content, in other words it is known that XC18 is more ductile than XC38 and XC48 because it contains less carbon, and XC38 is more ductile than XC48. Based on this fact we test the ductility approach and we have to prove this order of ductility values of XC18, XC38 and XC48 (Figure 15).

Experimental study of the ductility annealed iron and annealed copper

The tensile tests were performed on 03 samples of annealed iron

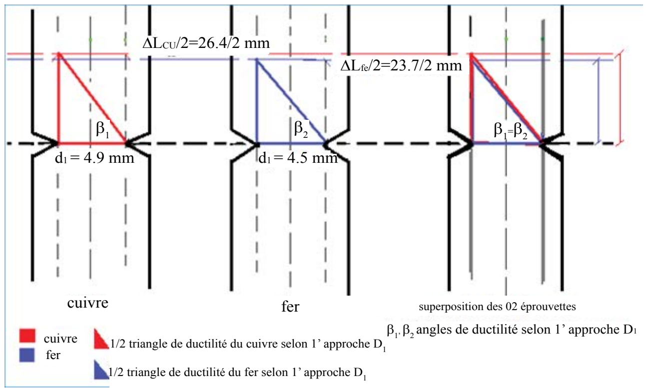

Figure 18: Geometric representation of the D_1 approach for annealing copper and annealed iron.

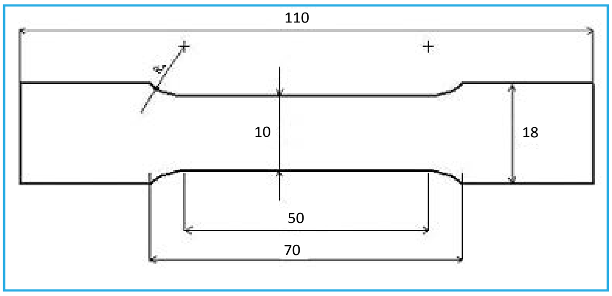

Figure 15: Specimen dimensions.

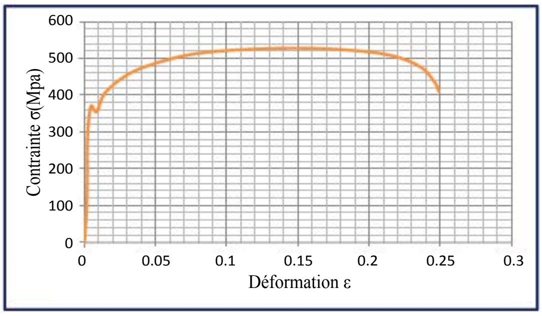

Figure 19: Tensile test curve of XC18.

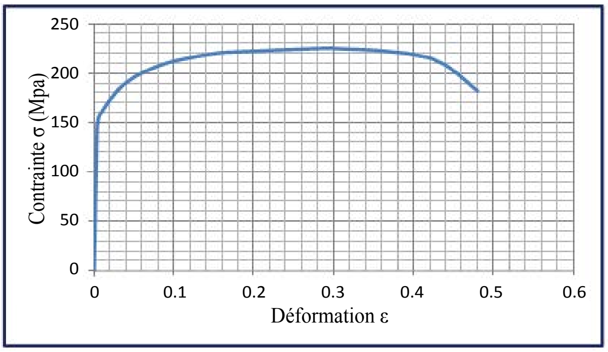

Figure 16: Tensile test curve of annealed iron.

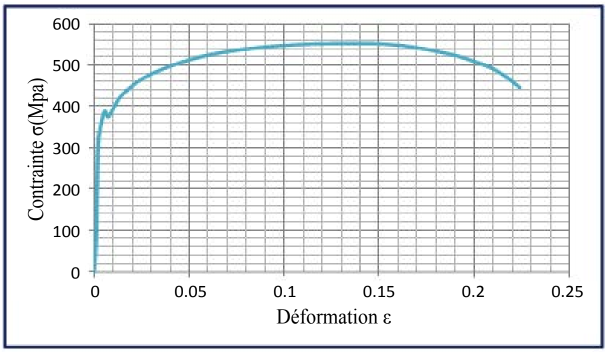

Figure 20: Tensile test curve of XC38.

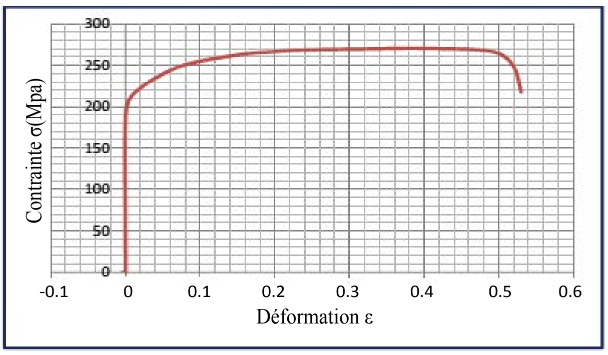

Figure 17: Tensile test curve of annealed copper.

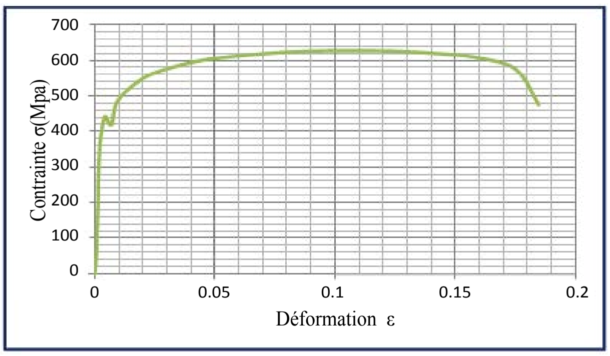

Figure 21: Tensile test curve of XC48.

Citation: Badreddine R, Abderrazak D, Kheireddine S (2016) New Approach of Metals Ductility in Tensile Test. J Appl Mech Eng 5: 225. doi: 10.4172/2168-9873.1000225

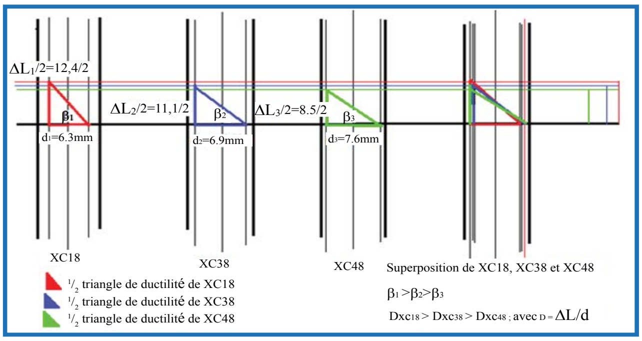

Figure 22: Geometric representation of the D_1 approach for XC18, XC38 and XC48.

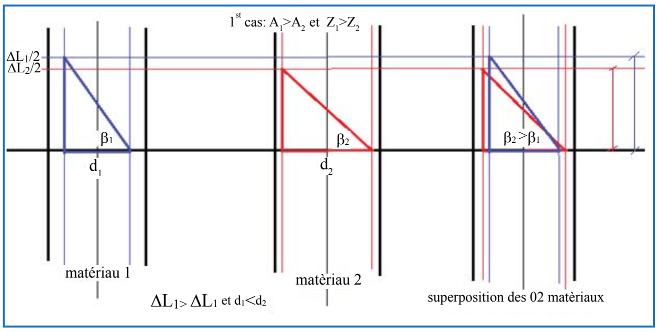

Figure 23: 1[st] case: $A_1>A_2$ et $Z1>Z_2$.

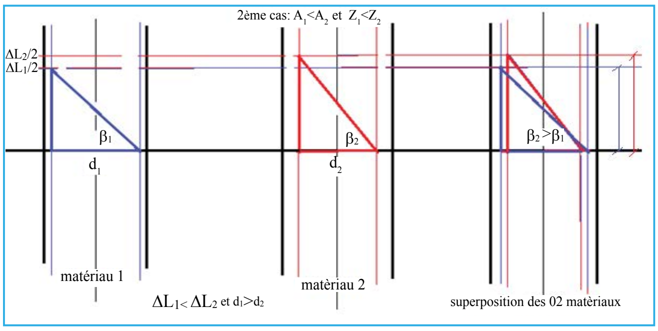

Figure 24: 2[nd] case: $A_1<A_2$ et $Z1<Z_2$.

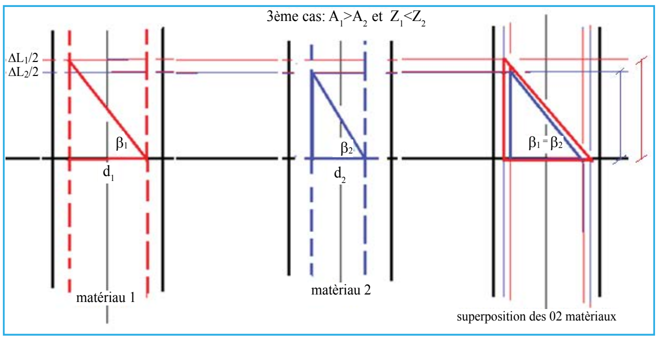

Figure 25: 3[rd] case: $A_1> A_2$ et $Z_1< Z_2$.

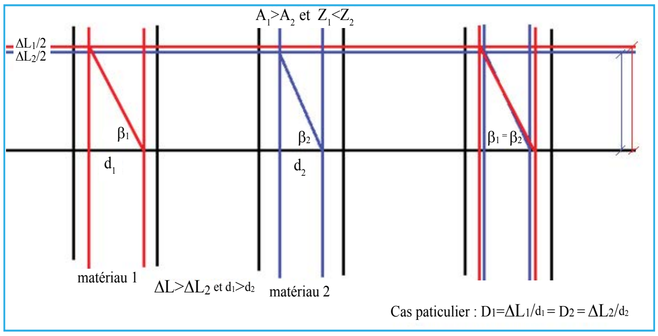

Figure 26: The 3[rd] possibility is a particular case.

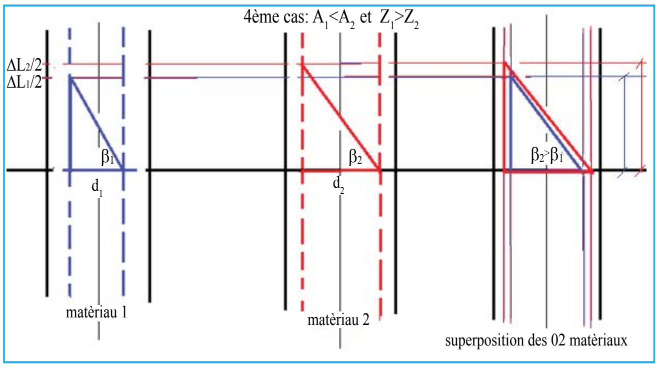

Figure 27: 4[th] case: $A_1< A_2$ et $Z_1 > Z_2$.

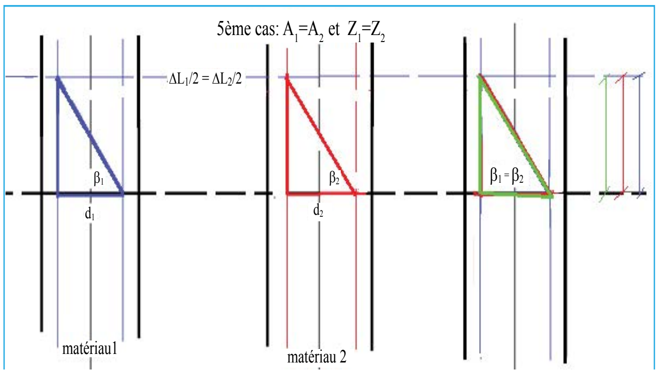

Figure 28: 5[th] case: $A_1 = A_2$ et $Z_1 = Z_2$.

Average Ductility $\sum \frac{X_i}{3}$	A%	Z%
Annealed Iron	47.5	79.9
Annealed Copper	52.8	76.2

Légend	Annealed Copper	Annealed Iron
$\Delta L_{moy} = \sum_{i=1}^{i=3} \frac{\Delta L_i}{3}$	26.4 mm	23.7 mm
$d_{1moy} = \sum_{i=1}^{i=3} \frac{d_{1i}}{3}$	4.9 mm	4.5 mm

Table 3: Comparative A, Z annealed iron and annealed copper.

Average Ductility	D1
Annealed Iron	5.3
Annealed Copper	5.4

Table 4: Experimental application of ductility modeling approach of annealed iron and annealed copper.

Légende	$A\% = \frac{L_0 - L_1}{L_0}$	$Z\% = \frac{\Delta S}{S_0}$	$D_1 = \frac{\Delta L}{d_1}$
Unit	%	%	Sans
Specimen 1	25.4	61.5	2
Specimen 2	25	60.3	1.9
Specimen 3	24	59	1.8
Calcul De La Moyenne $\sum \frac{X_i}{3}$	24.8	60.3	1.9

Table 5: Average values of A, Z and D_1 of XC18.

Légende	$A\% = \frac{L_0 - L_1}{L_0}$	$Z\% = \frac{\Delta S}{S_0}$	$D_1 = \frac{\Delta L}{d_1}$
Unité	%	%	Sans
Specimen 1	22.7	57.7	1.7
Specimen 2	22.2	50.9	1.6
Specimen 3	21.9	48.2	1.5
Calcul De La Moyenne $\sum \frac{X_i}{3}$	22.3	52.3	1.6

Table 6: Average values of A, Z and D_1 of XC38.

Légende	$A\% = \frac{L_0 - L_1}{L_0}$	$Z\% = \frac{\Delta S}{S_0}$	$D_1 = \frac{\Delta L}{d_1}$
Unité	%	%	Sans
Specimen 1	19.56	45.2	1.3
Specimen 2	17.24	39.1	0.9
Specimen 3	18.42	42.1	1
Calcul De La Moyenne $\sum \frac{X_i}{3}$	18.4	42.1	1

Table 7: Average values of A, Z and D_1 of XC48.

Paramètres De Ductilité	A%	Z%	D_1
Unité	%	%	Sans
XC18	24.8	60.3	1.9
XC38	22.3	52.3	1.6
XC48	18.4	42.1	1

Table 8: Values of A, Z and D_1 XC18, XC38 and XC48.

and annealed copper; we use the results of 03 curves we got, and then we exploited the Curve Unscan program to have the following average tensile curve for each metal (Figures 16-28).

Experimental study of the ductility of XC18, XC38 and XC48

It is shown in Tables 3-8.

General application of the approach, $D_1 = \frac{\Delta L}{d_1}$

In this case, we have 3 possibilities; most intéressant are:

Possibility 1 and 2: $\frac{\Delta L_1}{d_1} > \frac{\Delta L_2}{d_2}$

The 3rd possibility is a particular case:

With $\Delta L_1 \neq \Delta L_2$ et $\Delta d_1 \neq \Delta d_2$, we obtain:

$$\frac{\Delta L_1}{d_1} = \frac{\Delta L_2}{d_2}$$

Conclusion

Through this approach, we notice that D_1 is a valid and credible general parameter because its formula takes into account the longitudinal deformations using ΔL and the transverse deformations and transverse deformation across the necking diameter d_1. On the other hand the geometric representation of D_1 is interesting because it schematizes the ductility of materials using ductility triangle and ductility angle that we have presented.

References

1. Franz G (2008) Prédiction de la limite de formabilité des aciers multiphasés par une approche micromécanique. Engineering Sciences. Arts et Métiers Paris Tech.
2. Chastel Y (2006) Matériaux pour l'ingénieur.
3. Degallaix S (2006) Caractérisation des matériaux métalliques. 4. Feng ZQ (2011) Mécanique non linéaire MN91.
4. 4.Mathieu T (1750) Dissertation sur la ductilité des métaux, et les moyens de l'augmenter ETH-Bibliothek Zürich.
5. Mompiou F (2014) Des vermicelles dans les métaux. Centre d'élaboration des matériaux et d'études structurales CEMES-CNRS. Toulouse.
6. Poulain H D (2008) MA 41 Essai de traction. UTBM. Université de technologie de Belfort-Montbéliard.
7. ZhuY (2013) Mechanical properties of materials. NC State University. USA.
8. Berthaud Y (2004) Matériaux et proprieties.
9. Rollett AD, De Graef M (2007) Microstructure properties: I materials properties: strength ductility.
10. ADMET (2013) Sheet metal testing.
11. Jacquot B (2009) Propriétés mécaniques des. Biomatériaux utilizes en. Odontologie. Société Francophone de Biomatériaux Dentaires.
12. ASM (2004) American society for materials.
13. Montheillet F, Briottet L (2009) Endommagement et ductilité en mise en forme.
14. Beaucquis S (2012) Propriètés mécaniques des matériaux. Laboratoire SYMME Polytech'. IUT Annecy Département Mesures Physiques, France.
15. Bailon JP (2007) Des Matériaux, presses internationales polytechniques.
16. Chung BJ (2008) Film-wise and drop-wise condensation of steam on short inclined plates. J Mechanical Science and Technology 22: 127-133.
17. Jardin Nicolas H (2012) Essais des matériaux. Résistance des matériaux.
18. Dorlot JM (2000) Des matériaux. Propriétés mécaniques des métaux.
19. Ghomari F (2014) Sciences des matériaux de construction. Faculté des sciences de l'ingénieur. université aboubekr belkaid.
20. Dupeux M (2005) Aide-mémoire science des matériaux.
21. Zaiser M (2006) Scale invariance in plastic flow of cristalline solids. advphysics.
22. Thomas T (2006) Traité Matériaux métalliques.
23. Suquet P (2003) Rupture et plasticité.
24. Dorina N (2009) Matériaux et traitement. OFPPT Maroc.
25. Mandel J (1978) Propriétés mécanique des matériaux editions eyrolles.
26. Norme NF (2009) EN 10002, Essai de traction.
27. François D, Bailon JP (2005) Essais mécaniques des métaux Détermination des lois de comportement.

28. Charmet JC (1990) Mécanique du solide et des matériaux elasticité-plasticité-rupture école supérieure de physique et de chimie industrielles de paris paris tech - laboratoire d'hydrodynamique et mécanique Physique. France.

29. Anduze M (2013) Mécanique des détecteurs Du détecteur à la mesure. Institut National de Physique Nucléaire et de Physique des Particules, LLR - Laboratoire Leprince-Ringuet France.

30. Newey C, Weaver G (1990) Materials principles and practice.

31. Symonds J (1976) Mechanical properties of materials.

32. Charvet R (2009) Comportement à la traction de barres d'armature. Laboratoire de métallurgie mécanique école polytechnique. Fédérale de Lausanne.

33. Ben Tahar M (2005) Contribution a l'étude et la simulation du procède de l'hydroformage Engineering Sciences. Ecole Nationale Supérieure des Mines de Paris.

34. Strnadel B, Brumek J (2013) Effect of tensile test specimen size on ductility of R7T steel faculty of metallurgy and materials engineering Ostrava Tchécquie.

35. Brunet M (2011) Mécanique des matériaux et des structures.

36. Altmeyer G, Abed-Meraim F, Balan T (2013) Vue d'ensemble des relations théoriques entre la striction et les critères souches de localisation. Université de Lyon CNRS Laboratoire de Mécanique des Contacts et des Structures UMR5259 Insa de Lyon

37. Glowacki D, Kozakiewicz K (2013) Numerical simulation of the neck in heterogeneous material. Third international conference on material modelling. Warsaw University of technology, Varsovie Pologne.

38. Bueno R, Sánchez J, Rodríguez T (2009) New parameter for determining plastic fracture deformation of metallic materials. Department of Mechanics and Structures. University of Seville Spain Avenida Reina Mercedes 2 41012 Seville Spain.

39. Hosford WF (2010) Mechanical behaviour of materials. University of Michigan, USA.

40. Yasuyuki A (2010) Procédé de fabrication de fil d'acier japan.

41. Maya M (2008) Plasticité mise en forme. Arts et metiers – Paristech Centre d'enseignement et de recherche de Cluny. France.

42. Broniewski W (1938) Revue de métallurgie. Allongement de striction et travail de rupture la traction.

43. Blétry M (2007) Méthode de caractérisation mécanique des matériaux.

44. International standardization organization (ISO) (2009) EN-ISO-6892-1 October 2009 tensile test: mechanical properties.

45. Degoul PB (2010) Essai de traction. Etude des caractéristiques classiques I 1 Description de l'essai euro-norme 10002-I.

46. Chateigner D (2012) IUT Mesures Physiques Université de Caen Basse-Normandie Ecole nationale supérieure d'ingénieurs de Caen (ENSI CAEN) Laboratoire de cristallographie et sciences des matériaux (CRISMAT) Caen France.

47. Khalfallah A (2009) Fascicule de atelier de mécanique Institut supérieur des sciences appliquées et de technologie de sousse Tunisie.

48. Elias F (2013) Elasticité M2 Fluides Complexes et Milieux Divisés. Université Paris Diderot Paris France.

49. Col A (2011) Emboutissage des tôles, aspect mécanique Techniques de l'ingénieur BM7511.

50. Savoie J, Jonas JJ, Mac Ewen SR, Perrin R (1995) Evolution of r- value during the tensile déformation of aluminium textures and Microstructures 23: 1-23.

51. Abedrabbo N, Pourboghrat F, Crasley J (2006) Forming of aluminium alloys at elevated temperatures Part 1: Material characterization. Int J Plasticity 22: 314-341.

52. Prensier JL (2004) Les critères de plasticité: compléments.

53. Considère A (1885) Annales des Ponts et Chaussées 9: 574.

54. Swift HW (1952) Plastic instability under plane stress. J Mechanics and Physics of Solids 1: 1-18.

55. Hill R (1952) On discontinuous plastic states, with special reference to localized necking in thin sheets. J Mechanics and Physics of Solids 1: 19-30.

56. SAE (1989) Society for Automobile Engineers, USA.

57. Chomel P (2001) Sélection des matériaux métalliques Familles de matériaux.